



ELSEVIER

Superlattices and Microstructures 36 (2004) 21–29

Superlattices
and Microstructures

www.elsevier.com/locate/superlattices

Fabrication of highly oriented microstructures and nanostructures of ferroelectric P(VDF-TrFE) copolymer via dip-pen nanolithography

Qian Tang, San-qiang Shi*, Haitao Huang, Li Min Zhou

Department of Mechanical Engineering, The Hong Kong Polytechnic University, Hung Hom, Kowloon, Hong Kong

Available online 15 September 2004

Abstract

Microstructures and nanostructures of ferroelectric copolymer poly(vinylidene fluoride–trifluoroethylene) [P(VDF-TrFE)] are fabricated on gold via dip-pen nanolithography (DPN). The thickness of the patterns is about 1 nm after a critical concentration, regardless of the pattern scale. The polymer molecules are well orientated according to an all-*trans* conformation and have ferroelectric properties on the gold surface through electrostatic interaction, rather than the formation of chemical bonds. Increasing temperature has a positive effect on the growth rate of the P(VDF-TrFE). The electrostatic interaction between the P(VDF-TrFE) and the gold substrate and the intramolecular interaction of polymer molecules play important roles in the growth rate of the P(VDF-TrFE) patterns.

© 2004 Elsevier Ltd. All rights reserved.

1. Introduction

An AFM-based nanolithographic technique, dip-pen nanolithography (DPN), was developed by Mirkin and co-workers who used a coated atomic force microscopy (AFM) tip to deposit molecules on a substrate of interest [1]. It is a simple, low cost, and promising method for fabrication of nanostructures as compared with other nanotechnologies, such

* Corresponding author. Tel.: +852 2766 7821; fax: +852 2365 4703.
E-mail address: mmsqshi@polyu.edu.hk (S.-Q. Shi).

as photolithography, electron beam deposition. Nanostructures of biomolecules, magnetic materials, metallic oxide, and some polymers with special properties were fabricated via DPN directly or indirectly [2–4]. DPN was extended to electrochemical-DPN by applying a positive DC bias on the tip, in which an electrochemical reaction occurred [5]. These results imply that DPN has potential applications in the areas of advanced microelectronic devices, bio-analysis, and data storage, etc.

P(VDF-TrFE) exhibits the highest ferroelectric polarization and electromechanical response among known polymers, and has superior coupling compared with poly(vinylidene fluoride) (PVDF). It is widely used in the ultrasound industry as acoustic sensors and transducers [6–8], and is also used to form composite materials with piezoelectric ceramics (lead titanate) due to its flexibility and lower acoustic impedance compare with those of piezoelectric ceramics [9,10]. The methods used to deposit thin films of P(VDF-TrFE) are spin-coating and Langmuir–Blodgett deposition. Both methods are suitable for preparing bulk films, but not suitable for preparing nanostructures. Furthermore, the general method used to characterize the ferroelectric properties of P(VDF-TrFE) requires metallizing the thin film as the top electrode for poling. The result is good for thick films, while it is not suitable for thin films, because the metallization will affect the ferroelectric properties of thin films. AFM with a conductive tip as the top electrode can polarize and detect the ferroelectric properties nondestructively without metallization [11]. In the present study, structures on the microscale to nanoscale of P(VDF-TrFE) are fabricated on gold via DPN, and the mechanism for the deposition process is studied.

2. Experimental procedure

DPN patterning and AFM imaging were performed with a commercial AFM (Solver P47H, NT-MDT, Russia). The AFM system was placed in a homemade chamber. The typical spring constant, tip curvature radius, and resonance frequency of the silicon cantilever (a contact “golden” silicon cantilever, CSG11) used for DPN are about 0.03 N/m, 10 nm, and 10 kHz, respectively, from the NT-MDT company.

The substrate was prepared by sputtering a layer of 30 nm Au on top of a (100) silicon wafer with a Ti adhesion layer of 10 nm. The roughness of the polycrystalline gold film surfaces is about 0.6 nm, as determined from AFM.

In the DPN technique, the AFM tip is coated with a thin film of a chemical of interest. The chemical may be organic materials, biomolecules, or inorganic salt. The chemical molecules are deposited on the substrate surface during scanning with this coated tip or during the stay of the tip on the sample surface for a certain period of time. In the present study, 3.6 mg of P(VDF-TrFE) with a mole ratio of 80/20 (Piezotech S.A.) dissolved in 5 ml acetone was used as the ink. The silicon tip was coated by immersing the cantilever in the ink for 1 min, gently dried in air, and then used for DPN directly. DPN patterning was operated in contact mode with a contact force of 2.0 nN except when otherwise stated. The fabricated patterns were viewed via lateral force microscopy (LFM) images as well as the topography images with the coated tip. In order to avoid undesired deposition of P(VDF-TrFE), all the images were acquired at a high scanning rate of 500 $\mu\text{m/s}$.

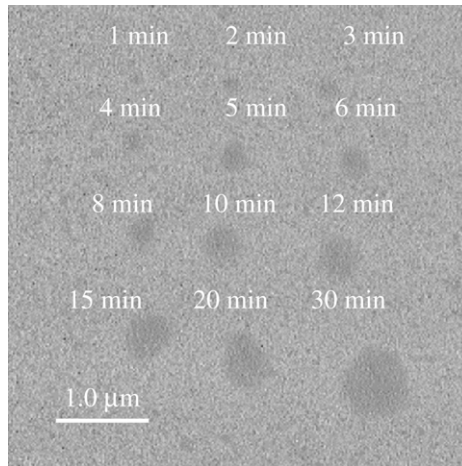


Fig. 1. A LFM image of point arrays written with different dwell times. Conditions: 22 °C, relative humidity 7%, contact force 2.0 nN. The tip coated with P(VDF-TrFE) was allowed to contact the gold substrate for 1, 2, 3, 4, 5, 6, 8, 10, 12, 15, 20, and 30 min, then the area was scanned at a rate of 500 $\mu\text{m/s}$. P(VDF-TrFE) point arrays with darker contrast were obtained. The diameters of the points increased with increasing duration.

3. Results and discussion

3.1. The influence of contact time and temperature

Fig. 1 shows a 5 by 5 μm lateral force microscopy (LFM) image of P(VDF-TrFE) point arrays written at different contact times. The P(VDF-TrFE) dark spots created via DPN can be clearly seen; the DPN was conducted at 22 °C and 7% relative humidity (RH). As compared with the gold substrate, the hydrophobic polymer layer of P(VDF-TrFE) provides a lower friction force to the AFM tip so a dark contrast appears in the LFM image, giving the same trend as ODT but with a much slower transfer rate [1]. The slower transfer rate was probably caused by the properties of the polymer and the interaction between the ink and the substrate. The size of the dot increases with the contact time.

Fig. 2 is the topography image obtained at the same time as the LFM image in Fig. 1. The areas covered with P(VDF-TrFE) exhibit brighter contrast, which means that these areas are higher than the neighboring areas. P(VDF-TrFE) cannot be clearly seen in topography images for short contact times, e.g., 1 and 2 min in Fig. 2. However, the LFM image (Fig. 1) gives black contrast, demonstrating that polymer was deposited on gold. On increasing the contact time to longer than 2 min, the polymer can be seen in the topography image. For 3, 4, and 5 min durations, the heights of the points are less than those of points obtained for longer durations. For much longer durations (longer than 5 min), the polymer patterns have the same height, about 1.0 nm, illustrating the uniformity of the P(VDF-TrFE) pattern formed on the gold. This result is similar to that for the formation of Self-Assembled Monolayers (SAM) of thiol on gold. At low concentrations, the alkane chains maximize their interaction with the gold surface by lying prone. The thiol molecules do not densely assemble themselves on the gold surface, resulting in low spatial resolution.

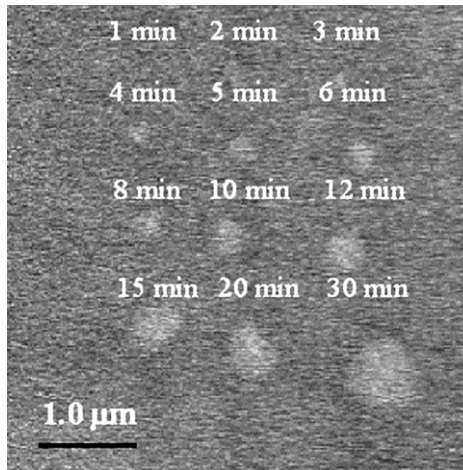


Fig. 2. The topography of point arrays written at different dwell times. Conditions: 22 °C, relative humidity 7%. The areas covered with P(VDF-TrFE) are higher than the neighboring areas. The topography image provides information of the P(VDF-TrFE) height on the gold substrate for fabrication via DPN.

When the concentration reaches a critical value, the thiol molecules assemble themselves densely and align on the gold surface, forming SAM [12–14]. Similarly, P(VDF-TrFE) deposited on the gold substrate is increasingly present and forms uniform patterns with increasing duration.

The dots formed at room temperature (22 °C) via DPN are not normal circles (Figs. 1 and 2); this is probably caused by the surface roughness. As described above, the transfer rate of P(VDF-TrFE) is slow, and the gold substrate prepared by sputtering is not ultraflat, with roughness ca. 0.6 nm. Both of these factors cause irregular circles in the LFM image (Fig. 1) and the topography image (Fig. 2). This can be overcome by increasing the transfer rate through increasing the temperature. Fig. 3(a) shows the LFM image of P(VDF-TrFE) dot arrays at different contact times obtained via DPN at 31 °C. The dots are regular circles and greater than those obtained at 22 °C (Fig. 1). The tests were repeated five times under the same conditions (i.e., with the same tip, fresh gold substrate, and the ink prepared at one time), and good repeatability was obtained. Fig. 3(b) shows the curve of contact time versus r^2 , where r is the dot radius. It can be found that r^2 scales linearly with the contact time. As stated above, P(VDF-TrFE) forms patterns on gold with uniform thickness after a critical concentration. It can be deduced that m (the mass of polymer deposited on gold) is proportional to the contact time. The tip coated with P(VDF-TrFE) can be thought of as a point source providing P(VDF-TrFE) without depletion during the DPN process.

In the gold–thiol system, a covalent Au–S bond is formed in the formation of SAM [15]. Thiols diffusing on gold and patterns formed via DPN were successfully explained with diffusion theory [16–19]. If the interaction between the ink molecules and substrate is greater than the intramolecular interaction between the ink molecules, the patterns formed via DPN are uniform, e.g., for ODT and MHA on gold [1]. Weak binding between the ink molecules and the substrate results in anisotropic patterns, where the diffusion is

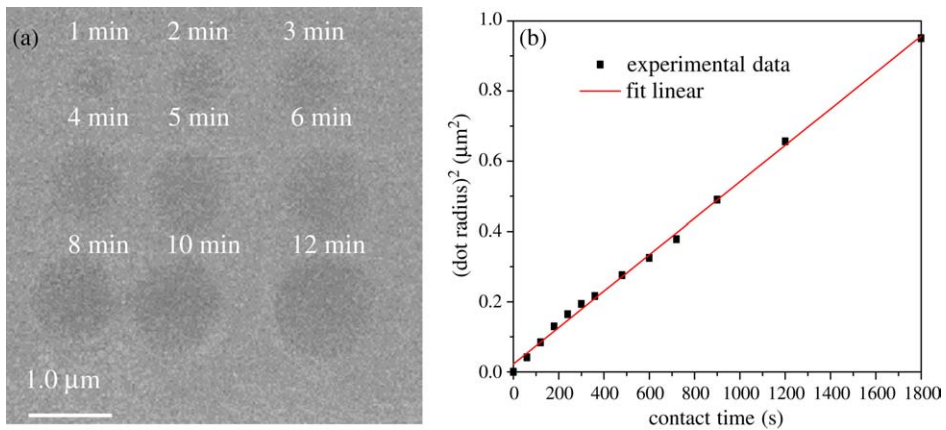


Fig. 3. A LFM image of P(VDF-TrFE) dot arrays at different contact times and the scaling analysis. (a) Conditions: 31 °C, relative humidity 7%, contact force 2.0 nN. The tip coated with P(VDF-TrFE) was allowed to contact the gold substrate for 1, 2, 3, 4, 5, 6, 8, 10, and 12 min, then the area was scanned at a rate of 500 $\mu\text{m/s}$. Dots with larger diameter were obtained compared with the case in Fig. 1(a). (b) Contact time versus (dot radius) 2 . r^2 scales linearly with the contact time.

dominated by the interaction between molecules [19]. In the gold–P(VDF-TrFE) system, the interaction between P(VDF-TrFE) and gold is probably electrostatic interaction. It is well known that the fluorine forms highly polar bonds with carbon, having a dipole moment $\mu = 6.4 \times 10^{-30}$ C m [20], and there are a positive part and a negative part in the molecule. This is the reason for most fluorinated polymers exhibiting ferroelectric properties. Gold, as a $4f^{14}5d^{10}6s^1$ transition metal, can provide electrons as donors resulting in electrostatic interaction between the positive part of P(VDF-TrFE) and gold.

3.2. XPS analysis

XPS was used to analyze the element contents and the gold valence on the surface. The sample was prepared by immersing the fresh gold substrate in an acetone solution containing P(VDF-TrFE) for 48 h, then taken out and rinsed with copious amounts of ethanol. A weak peak that emerged at 687.4 eV is shown in Fig. 4(a). It is the fluorine 1s characteristic peak, demonstrating that a thin polymer film self-adsorbed on the surface. Fig. 4(b) shows the Au 4f peak. The binding energy (83.7 eV) is almost equal to the binding energy (84 eV) of gold in its ground state. It can be concluded that the gold is in the metallic state. This demonstrates that the interaction between the polymer and the gold is an electrostatic interaction.

3.3. Detection of the ferroelectric response

The ferroelectric response was detected with the self-adsorbed P(VDF-TrFE) layer on the gold under AFM conditions. A varied DC voltage was applied between a conductive AFM tip and the sample to allow detection of the ferroelectric response. A circle was drawn by varying the voltage linearly from -10 V to $+10$ V counter-clockwise from point A as

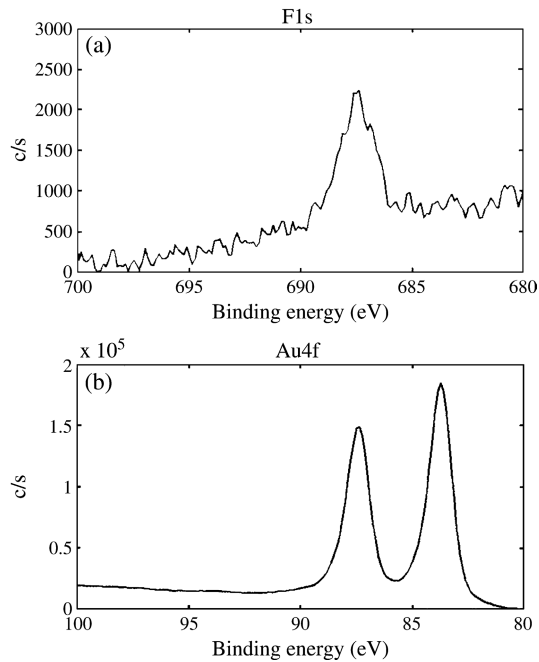


Fig. 4. The XPS result with Al $K\alpha$ radiation: (a) F 1s peak; (b) Au 4f peak.

shown in Fig. 5(a). When a positive voltage was applied to the tip, there was no apparent change in the sample, while a negative voltage produced a protruded pattern on the surface. The greater the voltage applied, the higher the protrusion obtained. The protruded pattern slowly returned to its original state. Fig. 5(b) shows the same pattern after 1 h. The result can be explained as resulting from the polymer absorbing on the gold according to a highly oriented, i.e., all-*trans* conformation and keeping the ferroelectric properties on the gold surface. Fig. 6 is a schematic diagram showing the uniform orientation of the P(VDF-TrFE) on the gold. The positive part of the P(VDF-TrFE) contacts with gold, while the negative part is positioned far from the gold and, therefore, a net dipole moment pointing from the upper part to the gold is formed. Similarly, the P(VDF-TrFE) oriented on the gold during DPN process and forms a pattern with the same thickness (about 1 nm). According to the Bune et al. report, the thickness of one layer of P(VDF-TrFE) is 0.5 nm [21]. The P(VDF-TrFE) patterns constructed via DPN should have two layers.

The result obtained by polarizing the self-adsorbed P(VDF-TrFE) layer can also be explained with hysteresis loops. Fig. 7 is a schematic diagram of the hysteresis loop for ferroelectric polymer [22]. In the left part the applied electric field is in the opposite direction to the molecular dipole moment. In the right part the electric field has the same direction as the molecular dipole moment. The upper half of the loop from A to A \ni in Fig. 7 shows that when negative voltages V_i ($i = 1, 2, 3$) are applied, the displacements appear with corresponding values H_i ($i = 1, 2, 3$). The higher the voltage applied, the greater the displacement obtained. In the right part, when a positive voltage is applied, the polymer

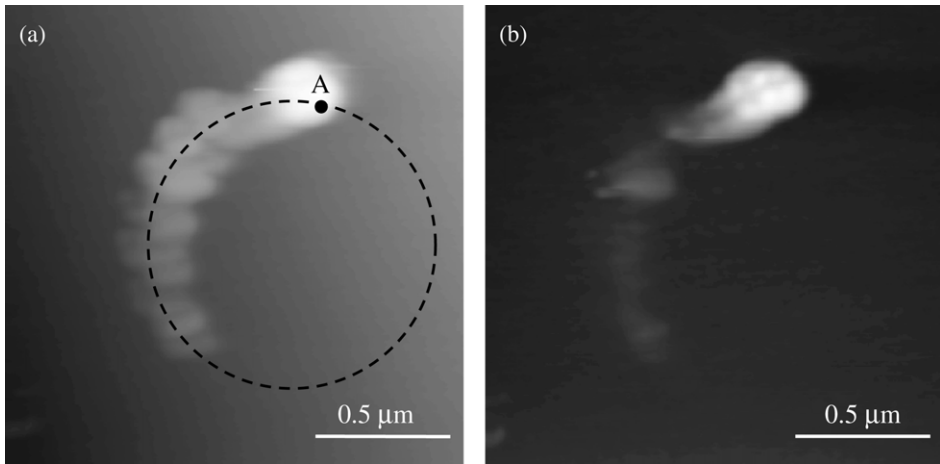


Fig. 5. The topography image obtained after applying a linearly varied DC voltage from -10 V to $+10$ V (between the tip and sample) to draw a circle from point A counter-clockwise in (a); there was no apparent change in the sample when a positive voltage was applied, while a negative voltage produced a protruded pattern on the surface. The greater the voltage applied, the higher the protrusion obtained. The protruded pattern slowly returned to its original state after a certain time; (b) is the image after 1 h.

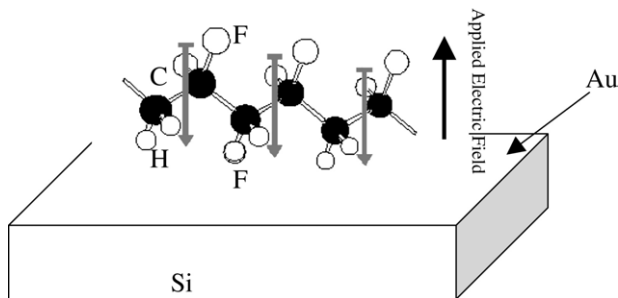


Fig. 6. A schematic diagram of the orientation of P(VDF-TrFE) on gold. The positive part of the P(VDF-TrFE) contacts with gold, while the negative part is positioned far from the gold and, therefore, a net dipole moment pointing from the upper part to the gold is formed.

changes along the curve $A \rightarrow O$, and no displacement can be obtained. In this study, we obtained a similar result by applying a varied voltage from -10 V to 10 V with AFM. There is no apparent change when a positive voltage is applied where the applied electric field has the same direction as the molecular dipole moment. When a negative voltage is applied on the tip, the direction of the applied electric field is opposite to the direction of the molecular dipole moment, as shown in Fig. 6, and a displacement is produced. This implies that the structures of the P(VDF-TrFE) constructed via the DPN possess ferroelectric properties.

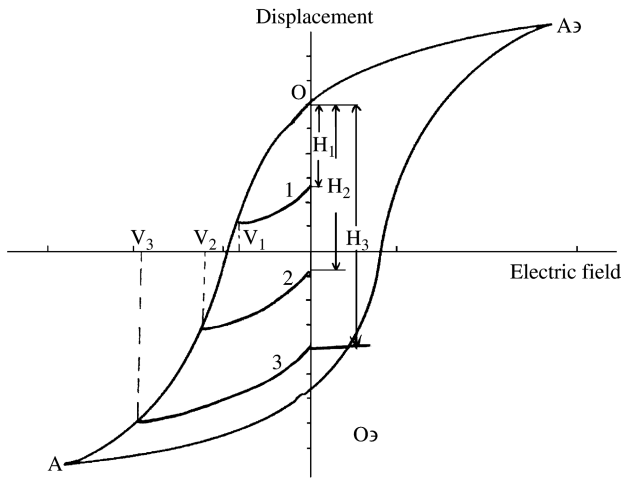


Fig. 7. A schematic diagram of the hysteresis loop for ferroelectric polymer. The upper half of the loop from A to A \ni shows that when negative voltages V_i ($i = 1, 2, 3$) are applied, the displacements appear with corresponding values H_i ($i = 1, 2, 3$). The higher the voltage applied, the greater the displacement obtained. In the right part, when a positive voltage is applied, the polymer changes along the curve A \ni O, and no displacement can be obtained.

4. Conclusions

In summary, we have, for the first time, successfully constructed the microstructures and nanostructures of a ferroelectric polymer, P(VDF-TrFE), on a gold substrate, via DPN. The molecules are well oriented (all-*trans* conformation) on the gold substrate, giving a uniform thickness (1 nm) regardless of the pattern scale after a critical concentration. The structures of the P(VDF-TrFE) have ferroelectric properties; this provides new opportunities for nanostructured sensor applications. It is also found that the temperature greatly affects the transfer rate of P(VDF-TrFE). The electrostatic interaction between the P(VDF-TrFE) and the gold substrate and the intramolecular interaction play important roles in the growth rate of P(VDF-TrFE) during the DPN process.

Acknowledgments

This work was funded by a research grant from the Hong Kong Polytechnic University (G-T687). The authors thank Professor C.A. Mirkin and Dr. David S. Ginger for providing valuable advice during the initial phase of this project.

References

- [1] R.D. Piner, J. Zhu, F. Xu, S. Hong, C.A. Mirkin, *Science* 283 (1999) 661.
- [2] (a) K.B. Lee, S.J. Park, C.A. Mirkin, *Science* 295 (2002) 1702;
 (b) H. Zhang, Z. Li, C.A. Mirkin, *Adv. Mater.* 14 (2002) 1472;
 (c) K.B. Lee, J.H. Lim, C.A. Mirkin, *J. Am. Chem. Soc.* 125 (2003) 5588;

- (d) X. Liu, L. Fu, S. Hong, *Adv. Mater.* 14 (2002) 231;
- (e) L. Fu, X. Liu, Y. Zhang, *Nano Lett.* 3 (2003) 757;
- (f) M. Su, X. Liu, C.A. Mirkin, *J. Am. Chem. Soc.* 124 (2002) 1560;
- (g) J.H. Lim, C.A. Mirkin, *Adv. Mater.* 14 (2002) 1474.
- [3] P. Amanda, J. Jang, G.C. Schatz, *Phys. Rev. Lett.* 90 (2003) 115505-1.
- [4] A. Noy, A.E. Miller, J.E. Klare, *Nano Lett.* 2 (2002) 109.
- [5] Y. Li, B.W. Maynor, J. Liu, *J. Am. Chem. Soc.* 123 (2001) 2105.
- [6] R. Schellin, G. Hess, W. Kuehnel, *IEEE Trans. Electr. Insul.* 27 (1992) 867.
- [7] M. Toda, *IEEE Trans. Ultrason. Ferroelectr. Freq. Control* 49 (2002) 299.
- [8] L. Paul, G. Michael, C. Grossman, *IEEE Trans. Ultrason. Ferroelectr. Freq. Control* 43 (1996) 536.
- [9] B. Ploss, F.G. Shin, H.L.W. Chan, *IEEE Trans. Dielectr. Electr. Insul.* 7 (2000) 517.
- [10] H.L.W. Chan, Q.Q. Zhang, W.Y.W. Ng, *IEEE Trans. Dielectr. Electr. Insul.* 7 (2000) 204.
- [11] P. Guthner, K. Dransfeld, *Appl. Phys. Lett.* 61 (1992) 1137.
- [12] D.K. Schwartz, *Annu. Rev. Phys. Chem.* 52 (2001) 107.
- [13] E.D. Pylant, G.E. Poirier, *Science* 272 (1996) 1145.
- [14] G.E. Poirier, W.P. Fitts, J.M. White, *Langmuir* 17 (2001) 1176.
- [15] R.G. Nuzzo, D.L. Allara, *J. Am. Chem. Soc.* 105 (1983) 4481.
- [16] J. Jang, S. Hong, G.C. Schatz, *J. Chem. Phys.* 115 (2001) 2721.
- [17] P.V. Schwartz, *Langmuir* 18 (2002) 4041.
- [18] P.E. Sheehan, L.J. Whitman, *Phys. Rev. Lett.* 88 (2002) 156104-1.
- [19] P. Manandhar, J. Jang, G.C. Schatz, *Phys. Rev. Lett.* 90 (2003) 115505-1.
- [20] A.J. Lovinger, *Science* 220 (1983) 1115.
- [21] A.V. Bune, V.M. Fridkin, S. Ducharme, *Nature* 391 (1998) 874.
- [22] H.S. Nalwa, *Ferroelectric Polymers*, Marcell Dekker, Inc., New York, 1995.